Cold Regions Science and Technology 104–105 (2014) 7–13

Contents lists available at ScienceDirect

Cold Regions Science and Technology

journal homepage: www.elsevier.com/locate/coldregions

Laboratory study on the adhesive properties of ice to the asphalt pavement of highway

Han-Cheng Dan [a,b,c], Lin-Hua He [a], Jin-Feng Zou [a,*], Lian-Heng Zhao [a], Shi-Yao Bai [b,c]

[a] School of Civil Engineering, Central South University, Changsha, Hunan 410075, China
[b] Post-doctoral Research Center, Guizhou Transportation Planning Survey & Design Academe, Guiyang, Guizhou 550001, China
[c] National Engineering Laboratory for Mountain Traffic Disaster Prevention and Control Technology (Guizhou), Guiyang, Guizhou 550001, China

ARTICLE INFO

Article history:
Received 23 September 2013
Accepted 11 April 2014
Available online 4 May 2014

Keywords:
Ice adhesion
Asphalt pavement
Adhesive strength
Ice temperature
Texture depth

ABSTRACT

Currently, there are few quantitative studies on the adhesion of ice to the asphalt pavement surface. In this paper, a large-scale freezing laboratory is employed to simulate the low-temperature and wet environment, and a full-scale asphalt pavement model is constructed in the freezing laboratory. The experimental schemes are developed to measure the magnitudes of the normal and horizontal adhesive force of ice to the rough asphalt pavement surface. Then, the normal and horizontal adhesive strength of ice is evaluated to quantify the adhesive force per unit rough area, and the effects of ice temperature as well as the mean texture depth of asphalt pavement on the ice adhesive strength are taken into consideration. Based on the test and evaluation results, it is found that the normal and horizontal ice adhesive strength increases with the ice temperature decrease. The adhesive strength in the normal direction exhibits a logarithmic relation to the ice temperature whereas that in the horizontal direction shows a linear relation. The adhesive strength of ice to the asphalt pavement with higher mean texture depth (0.65 mm) is stronger than that with the lower mean texture depth case (0.50 mm).

1. Introduction

The adhesion of ice to variable materials is a significant concern in civil, power grid facilities and aeronautical structures exposed to low-temperature environments (Laforte and Beisswenger, 2005; Loughborough, 1946; Petrenko, 1998). The icing formed on the surface of civil structures exerts adverse impacts on the engineering construction and normal use (Hanbali, 1994). It is well known that the wet asphalt pavement is more likely to be frozen in the low-temperature environment especially in a moist mountain area. Thereinto, the area in western China often suffers from the freezing rain during the winter; and the ice on the asphalt pavement reduces the pavement skid-resistance and subsequently endangers the traffic safety (Gustafson, 1982; Zhu et al., 2012). Accordingly, the techniques (e.g., anti-freezing coating, deicing products and mechanical deicing) were developed and applied to reduce this kind of adverse impact (Croutch and Harttey, 1992; Petrenko, 1999; Sarkar and Farzaneh, 2009). The adhesion strength of ice directly affects the difficulty and effectiveness of deicing, and indirectly affects the choice of deicing techniques (Oksanen, 1983; Tan, 2008). So far, there are few researches which quantify the ice adhesion to the asphalt pavement surface under different cold conditions. Nonetheless, relatively more investigations have been presented to measure and calculate the adhesion of ice to the certain materials in the other research fields (Andrews and Lockington, 1983; Raraty and Tabor, 1958; Ryzhkin and Petrenko, 1997).

Raraty and Tabor (1958) studied the adhesion and strength properties of ice to variable solid surfaces and compared the differences of the adhesion of ice to polymeric materials and metals. Ryzhkin and Petrenko (1997) studied an electrostatic model of ice adhesion based on the existence of the surface states of protonic charge carriers on the surface of ice. Their work provides an understanding of the time- and temperature-dependent phenomena that explain the difference between the adhesive properties of ice and water. Andrews and Lockington (1983) developed a test method to study the properties of ice adhering to the substrates of stainless steel, titanium and anodized aluminum under different low temperatures. Laforte et al. (2002) presented the adhesion reduction efficiency of seven solid ice phobic coatings. The results were analyzed in terms of ice density, hydrophobic properties of the coatings, and roughness surface characteristics. Dotan et al. (2009) carried out the ice adhesion tests and measured the contact angle to establish the relationship between water wetting and ice adhesion. Yang and Jin (2002) reviewed the ice adhesion phenomenon under sub-freezing temperature in terms of the freezing condition, adhesive properties, the method and technology to reduce the adhesion of ice. Based on the experimental data for the adhesion stress of ice to the surface of metal and non-metal materials, the freezing adhesion stress is independent of the contact area and ice thickness. In

* Corresponding author. Tel.: +86 13873105859.
E-mail addresses: danhancheng@csu.edu.cn (H.-C. Dan), linhuahe_csu@163.com (L.-H. He), zoujinfeng_csu@163.com (J.-F. Zou), zlh8076@163.com (L.-H. Zhao), baishiyao137@sina.com (S.-Y. Bai).

http://dx.doi.org/10.1016/j.coldregions.2014.04.002
0165-232X/

addition, some researchers reported the adhesion force of ice to the structure surfaces (Baker et al., 1962; Chu and Scavuzzo, 1991; Hassan et al., 2010; Maeno, 2004; Matsumoto and Kobayashi, 2007; Yang et al., 2004); however, most of these studies are restricted to the field of material engineering and sporadic or even no concern has been raised in pavement engineering. The asphalt pavement is porous with a rough surface which is different from other materials (e.g., the metal, plastics, polymeric material and other materials with a smooth surface). It is understandable that the freezing mechanism of ice on the electric wires, airplane wings and some metal materials is largely different from that on the asphalt pavement surface due to their distinct material properties. Consequently, the study method cannot be directly applied, and the relevant conclusions may be different in the pavement engineering. Therefore, the specific and targeted fundamental experimental studies are needed.

For the asphalt pavement frozen in low temperature and wet environment, the adhesive strength of ice to the pavement is generated. It includes normal (perpendicular to the interface) and horizontal (parallel to the interface) adhesive strength which characterizes the strong and weak of adhesive force per unit rough contact area. In this paper, a large-scale freezing laboratory is employed to simulate the low-temperature and wet environment, and a full-scale asphalt pavement model is constructed in the freezing laboratory. Experimental schemes are developed to measure the ice adhesion and quantificationally analyze the effects of ice temperature and pavement surface texture on the adhesive strength of ice to the asphalt pavement surface.

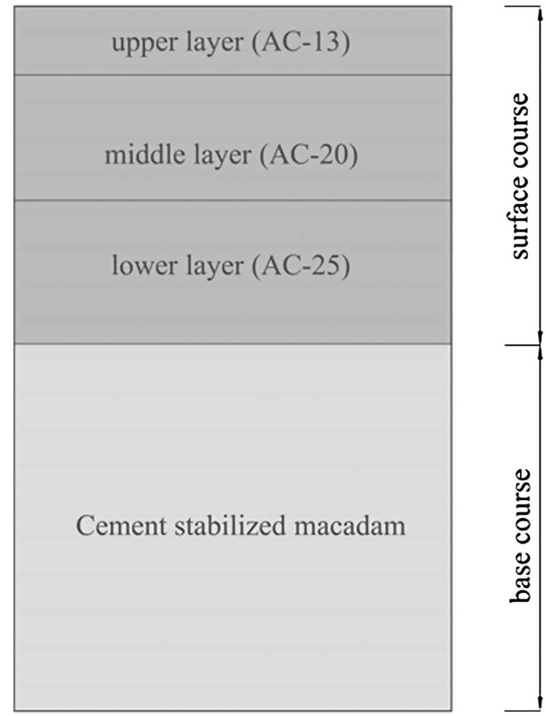

Fig. 1. Schematic diagram of the pavement structure.

2. Experimental

2.1. Introduction to large-scale freezing laboratory

2.1.1. Experimental environment simulation

The ice is essentially formed in a wet and low temperature environment. The large-scale freezing laboratory is constructed for simulating this kind of environment. The air temperature, rainfall, wind speed and pavement temperature can be controlled. The technical parameters of the laboratory with respect to the environment are listed in Table 1.

2.1.2. Pavement structure and test model

The pavement structure is shown in Fig. 1 and the experimental model is filled with building materials (asphalt mixture) (Fig. 2). The experimental model is constructed in the freezing laboratory and subjected to low temperature and wet condition. Platinum sensors are buried in the upper surface course and put on the pavement top surface to detect temperature variation during the temperature drop in the laboratory.

2.2. Test instruments and specimens

2.2.1. Normal adhesion test

The normal adhesion of ice to the asphalt mixture can be weighed by the adhesive force at the irregular interfaces. It is much difficult, if not impossible, to directly pull out the ice from the pavement surface because of the difficult operation. In this paper, we adopt the cylinder specimen (standard Marshall specimen with diameter 102.2 mm and height 63.5 mm) casted with the asphalt mixture which is the same as the material of the pavement surface course (Fig. 3). The cylinder specimen is laid on the pavement surface, and the water between specimen and pavement surface can be frozen under a low temperature condition. If an instrument can be utilized to pull the specimen upward till the specimen separates from the pavement surface, the force obtained by the instrument should be regarded as the adhesive force at the interface of ice and asphalt mixture, no matter the interface is at the ice and pavement surface or the ice and specimen.

To facilitate the test, the combination specimen consists of the cylinder specimen and metal block which is fixed on the specimen with screws to connect to the pull-off tester. The pull-off tester can pull out the specimen from the freezing pavement surface (Fig. 4 shows the schematic diagram for testing the normal ice adhesive force to the asphalt pavement surface.).

2.2.2. Horizontal adhesion test

The specimen for the horizontal adhesion test is also the standard Marshall specimen (Fig. 3) without connecting the metal block. The device to provide a push force is named push-off tester and the schematic diagram is shown in Fig. 5. It can provide about 100 kN maximum push force with an accuracy of 0.01 kN. The push-off tester can record the peak value of the push force when the specimen is pushed away from the pavement surface.

2.2.3. Mean texture depth (MTD) of asphalt pavement and specimen

Texture is a surface characteristic which influences the pavement functional quality significantly (e.g., skid resistance performance) (Flintsch et al., 2007; Zou et al., 2011). Surface macrotexture is a predominant contributor to pavement roughness and skid resistance (Ahammed and Tighe, 2011; Ongel et al., 2009). In this paper, the mean texture depth (MTD) is selected for characterizing the surface roughness of asphalt pavement. After the asphalt pavement being paved, the MTD (macrotexture) is measured through sand patch

Table 1
Environment technical parameters of the large-scale freezing laboratory.

Internal spatial dimension (m)	Air temperature (°C)	Pavement temperature (°C)	Humidity	Rain flow (Th^{-1})	Wind speed (ms^{-1})
3 × 9 × 2.7(W × D × H)	−10–60	−10–60	<100%	<25	1.0–17

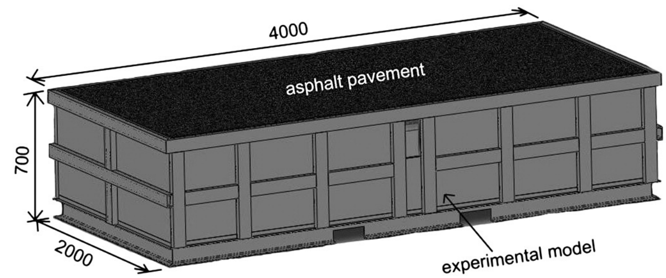

Fig. 2. Schematic diagram of the pavement model.

method (MoTPRC, 2012). In general, there are areas of the pavement surface with different compaction degrees, and the surface roughness is thus different (i.e., the MTD of the pavement surface is different). Two typical classifications of the obviously different roughness areas (I and II classifications) are measured (Table 2). Moreover, the specimens are casted with the approximate MTD through adjusting the compaction degree of the mixture. Three specimens for each classification are casted and the MTDs are measured (Table 2).

2.3. Test scheme and procedures

2.3.1. Normal adhesion test

The test method is designed to test the normal adhesive force of ice to the pavement. Firstly, the air temperature of the freezing laboratory falls down to the target temperature and keeps constant. Then, the combination specimen is placed in the low temperature environment. Under this condition, the pavement surface is wetted by spraying the water and wet specimens are put on the pavement surface (the MTDs of specimen and pavement are essentially the same). After water being frozen, the pull-off tester is placed on the right position and connected to the combination specimen. Then, the tester slowly provides the upward pull force (50 N/s) till the specimen separates from the pavement surface (quasi-static loading). During this time, the pull force will reach the maximum value and the value can be saved in the tester storage. Then, the tester is unloaded. It is significant that the platinum temperature sensor is quickly plugged into the specimen bottom to measure the ice temperature in the process of unloading. Three specimens are classified as a test set and three maximum pull force values are recorded. Fig. 6 illustrates the scene pictures for testing the normal ice adhesive force. Picture *A* is the process of quasi-static loading; picture *B* is the specimen breaking away from icing pavement; picture *C* shows the bottom of specimen after test and picture *D* shows the ice marks on pavement after test).

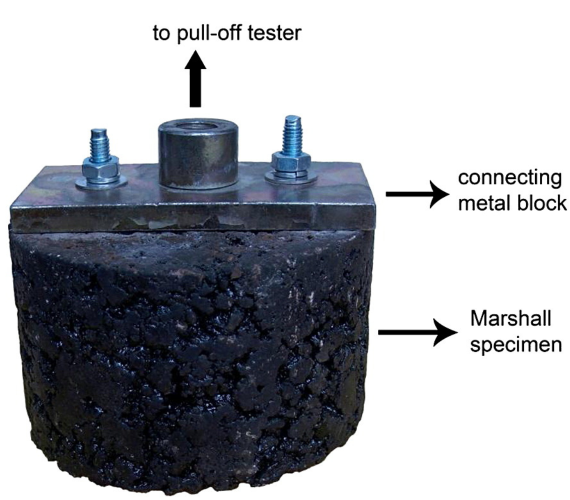

Fig. 3. Picture of combination specimen for testing the normal adhesive force.

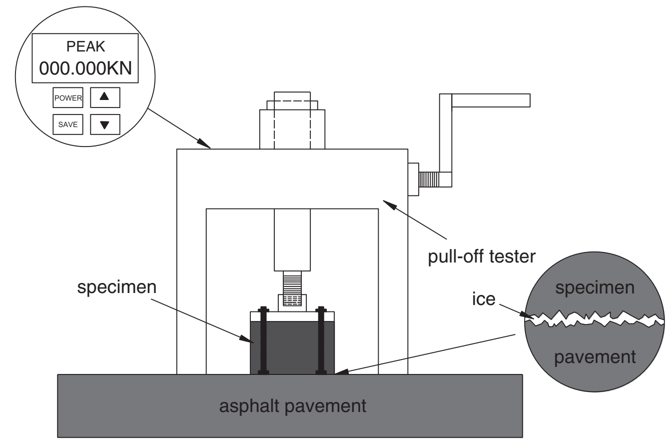

Fig. 4. Schematic diagram for testing the normal ice adhesive force to the asphalt pavement.

It is worth noting that the accurate contact area between the specimen and the asphalt pavement cannot be measured accurately because those surfaces are rough and hackly. In addition, the irregularities of the surfaces are distributed randomly. Therefore, the experiment in this paper can only measure the adhesive force between the interfaces. The adhesive strength is the adhesive force per unit rough area. In this paper, the specimen base area with the MTD is used to characterize the rough surface of the asphalt pavement and to represent the contact area. Accordingly, the evaluated adhesive strength is representative and comparable in terms of considering the effect of the MTD of the pavement surface.

2.3.2. Horizontal adhesion test

First of all, the freezing laboratory keeps the inner space under a low temperature condition. The Marshall specimens are put in the environment till the temperature falls down to certain minus centigrade (target temperature). Then, the test area on the asphalt pavement is wetted by spraying sufficient water which is frozen to generate the bonding force between the specimen bottom and pavement surface in the cold environment. After the specimens being put on the pavement and undergone the freezing process for a sufficient time, the ice is formed and maintained stable. Then, the ice around the edge of the specimen bottom is cleaned to eliminate the undesired resistance force during the push process. The push-off tester is then placed on the pavement and spaced a little distance between the piston top and specimen (Fig. 5). Next, the tester slowly provides a push force at a slow speed (50 N/s), and the piston top will approach and contact the specimen side face till the specimen is pushed away from pavement surface (quasi-static loading). At this time, the push force will reach the maximum value which can be recorded and saved. Three specimens are used for one test set and the average value of push forces can be obtained to represent the test result. Fig. 7 illustrates the scene pictures for testing the horizontal ice adhesive force. Picture *A* is the process of quasi-static loading; picture *B* shows the specimen bottom and ice marks after test and picture *C* shows the ice temperature measurement with temperature sensor).

Likewise, the specimen bottom area is used to calculate the horizontal adhesive strength of ice to the asphalt pavement.

3. Results and discussions

3.1. Normal adhesive property

For the MTD with the values of 0.50 mm and 0.65 mm, 24 and 19 set tests are conducted respectively and the test data are collected. The

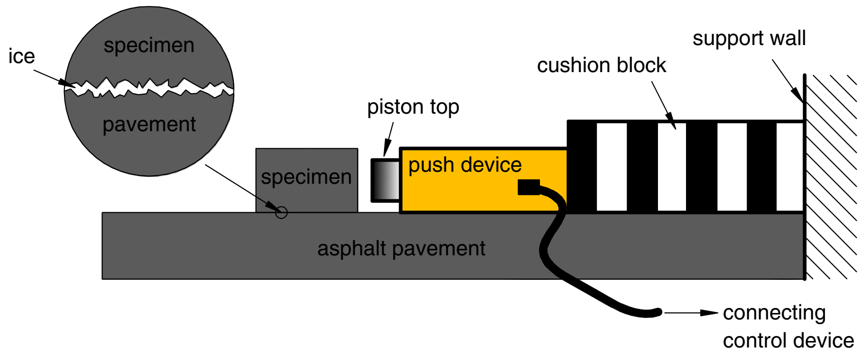

Fig. 5. Schematic diagram for testing the horizontal ice adhesive force to the asphalt pavement.

scatter diagrams corresponding to the normal adhesive strength of ice (NASI) and ice temperature are shown in Figs. 8 and 9 respectively.

Through the least-square fit method, the relationship between the ice temperature and NASI can be approximately in a logarithmic manner. The relationship can be given as the following formula

$$f_{nad} = a_1 \ln(-T_{ice}) + b_1 \tag{1}$$

where f_{nad} is the normal adhesive strength of ice (NASI) to the pavement surface, kPa; T_{ice} is the value of ice temperature, °C; and a_1 and b_1 are the fitting parameters.

Since the MTDs of the test specimens are slightly different (Table 2), the difference between the fit curves is slight which can be found in Figs. 8 and 9. That is to say, a slight variation of MTD results in little difference of NASI to the pavement under the same ice temperature condition. In order to detect the effect of large variation of the MTD on the NASI, the comparisons are conducted in terms of the MTD, which is 0.50 mm and 0.65 mm. According to the fitting equation and test results, the expressions for the two cases are given by Eqs. (2) and (3), and the comparison diagram is shown in Fig. 10.

$$\begin{cases} f_{nad} = 201.48 \ln(-T_{ice}) + 358.33 \\ R^2 = 0.9731 \end{cases} \text{as pavement } \textbf{MTD} \text{ is } 0.50 \text{ mm} \tag{2}$$

$$\begin{cases} f_{nad} = 223.65 \ln(-T_{ice}) + 375.26 \\ R^2 = 0.9909 \end{cases} \text{as pavement } \textbf{MTD} \text{ is } 0.65 \text{ mm} \tag{3}$$

In Eqs. (2) and (3), the relation coefficients are 0.9731 and 0.9909 respectively. It indicates that the logarithmic curve can well appropriate the variation of ice adhesion on the pavement under different low temperature conditions.

It also can be seen from Fig. 10 that the NASI increases with the decreasing ice temperature for the MTD that is either 0.50 mm or 0.65 mm. For the case that the MTD is 0.50 mm, the NASI increases from 82.4 kPa to 758 kPa when the ice temperature changes from −0.2 °C to −7 °C; while the MTD is 0.65 mm, the NASI increases from 186 kPa to 844.4 kPa when the ice temperature changes from −0.4 °C to −8.1 °C. Furthermore, the ice temperature changes from 0 °C to −2 °C, and the increase gradient of adhesive strength (NASI) is sharper than that ranging from −2 °C to −8 °C. Overall, the NASI of the asphalt mixture with 0.65 mm MTD is larger than that with 0.50 mm. The adhesive strength (NASI) improvement between the two cases can be quantified according to Eqs. (2) and (3) and given by

$$\delta_1 = \frac{223.65 \ln(-T_{ice})\text{-}201.48 \ln(-T_{ice}) + 16.93}{201.48 \ln(-T_{ice}) + 358.33} \times 100\% \tag{4}$$

where δ_1 represents the improvement percentage of NASI for the case when the MTD is 0.65 mm compared to when it is 0.50 mm, %.

For the ice temperature varying from −0.5 °C to −8 °C, the improvement of δ_1 grows from 0.7% to 8.1% (Fig. 11). It also can be seen from Fig. 11 that the NASI improvement grows up rapidly at the relative high ice temperature (below the water freezing point temperature) and tends to be approximately stable for the ice temperature that is increasingly lower.

3.2. Horizontal adhesive property

When the MTD is 0.50 mm and 0.65 mm, 30 and 28 set tests are conducted respectively, and the test data are collected. The scatter diagrams corresponding to the horizontal adhesive strength of ice (HASI) and ice temperature are shown in Figs. 12 and 13 respectively.

Through the least-square fit method, the relationship between the ice temperature and HASI is nearly linear which can be approximated by the following equation

$$f_{had} = a_2 T_{ice} + b_2 \tag{5}$$

where f_{had} is the horizontal adhesive strength of ice (HASI) to the pavement surface, kPa; T_{ice} is the value of ice temperature, °C; and a_2 and b_2 are the fitting parameters.

Accordingly, the fit curve expressions for the relationship between the ice temperature and HASI based on the test data can be given below

$$\begin{cases} f_{had} = -127.74 T_{ice} + 13.337 \\ R^2 = 0.985 \end{cases} \text{when pavement } \textbf{MTD} \text{ is } 0.50 \text{ mm} \tag{6}$$

$$\begin{cases} f_{had} = -133.52 T_{ice} + 38.666 \\ R^2 = 0.9884 \end{cases} \text{when pavement } \textbf{MTD} \text{ is } 0.65 \text{ mm} \tag{7}$$

In Eqs. (6) and (7), the relation coefficients are 0.985 and 0.9884 respectively. It indicates that the linear expression in Eq. (5) can describe the variation of HASI of the asphalt pavement very well under different low temperature conditions.

It can be seen from Fig. 12 that the HASI increases linearly with the drop of ice temperature when the MTD is 0.50 mm and 0.65 mm

Table 2
The MTD of specimen and pavement surface.

Surface types		Specimen 1#	Specimen 2#	Specimen 3#	Pavement
MTD (mm)	I	0.50	0.52	0.51	0.50
	II	0.63	0.66	0.66	0.65

Fig. 6. Scene pictures for testing the normal ice adhesive force (A. quasi-static loading; B. specimen breaking away from icing pavement; C. bottom of specimen after test; D. ice marks on pavement after test).

respectively. For the case when the MTD is 0.50 mm, HASI increases linearly from 166.4 kPa to 778.3 kPa when the ice temperature changes from −0.9 °C to −6.1 °C; while when the MTD is 0.65 mm, the HASI grows up linearly from 42.8 kPa to 971.7 kPa for the ice temperature ranges from −0.3 °C to −7.3 °C. Furthermore, the difference between the two cases can be obviously found. Overall, the HASI of the pavement

Fig. 7. Scene pictures for testing the horizontal ice adhesive force (A. quasi-static loading; B. specimen bottom and ice marks after test; C. ice temperature measurement).

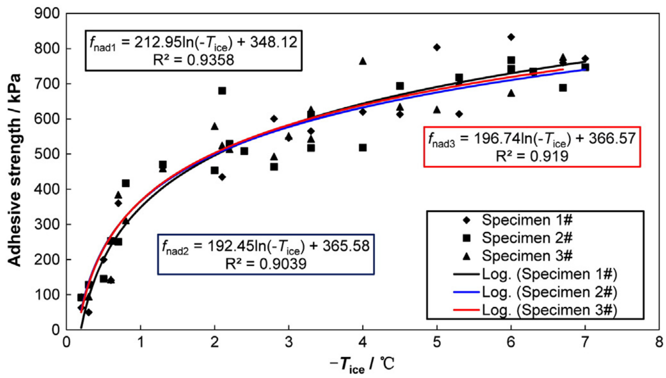

Fig. 8. Relationship between ice temperature and normal ice adhesive strength (the pavement MTD is about 0.50 mm).

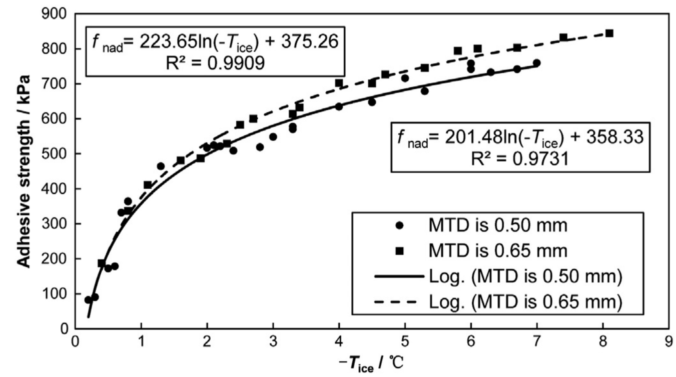

Fig. 10. Comparison of the relationship between ice temperature and normal ice adhesive strength for different pavement MTDs.

with 0.65 mm MTD is larger than that of the pavement with 0.50 mm MTD. The quantitative difference for the variable ice temperatures can be defined by

$$\delta_2 = \frac{-5.78T_{\text{ice}} + 25.329}{-127.74T_{\text{ice}} + 13.337} \times 100\% \tag{8}$$

where δ_2 represents the improvement percentage of HASI for the MTD of 0.65 mm compared to that of 0.50 mm, %. The relationship between δ_2 and T_{ice} is shown in Fig. 13.

It can be seen from Fig. 13 that the improvement of δ_2 falls down rapidly with the decreasing ice temperature, and it tends to be gentle when the ice temperature becomes lower. For instance, the improvement of δ_2 falls from 36.5% down to 6.9% and tends to be stable when the temperature changes from −0.5 °C to −8 °C (Fig. 13).

4. Concluding remarks

In this paper, a large-scale freezing laboratory was introduced into the experiment, which can simulate the low-temperature and wet environment, and an asphalt pavement model was constructed according to the full-scale pavement structure. The test schemes were developed to measure the magnitudes of the normal and horizontal adhesive forces of ice to the asphalt pavement with variable mean texture depths under different ice-temperature conditions. The magnitudes of adhesive strengths (normal and horizontal) were evaluated and the relationships between the ice temperature and adhesive strengths were illustrated through the least-square fit method. Furthermore, the different mean texture depths of the pavement surface were taken into consideration and the comparisons were carried out. Accordingly, the conclusions can be drawn as follows:

(1) The normal adhesive strength of ice increases in an approximately logarithmic relation with the decrease of the ice temperature.
(2) The normal adhesive strength of ice to the asphalt pavement with higher mean texture depth (0.65 mm) is larger than that with lower mean texture depth case (0.50 mm). When the ice temperature varies from −0.5 °C to −8 °C, the improvement of normal ice adhesive strength grows from 0.7% up to 8.1% and then tends to be stable.
(3) The horizontal adhesive strength of ice increases with the decreasing ice temperature and the relationship between them is approximately linear.
(4) Compared to the lower mean texture depth case (0.50 mm), the horizontal adhesive strength of ice has a larger value to the asphalt pavement with a higher mean texture depth (0.65 mm). The improvement of the horizontal ice adhesive strength falls down from 36.5% to 6.9% and tends to be stable when the temperature changes from −0.5 °C to −8 °C.

As mentioned earlier in the paper, the use of the specimen bottom area leads to the difference in evaluating the adhesive strength of ice to the asphalt pavement surface. This difference basically comes from the complex microstructure of the pavement surface and it is very difficult to measure the exact contact area between the ice and pavement surface. There are many convex–concave microstructures randomly distributing on the pavement surface; therefore, the actual contact area may be larger than that of specimen bottom.

Actually, the apparent area of the rough pavement, even though it can be tested exactly, is not the exact ice contact area. Figs. 6 and 7

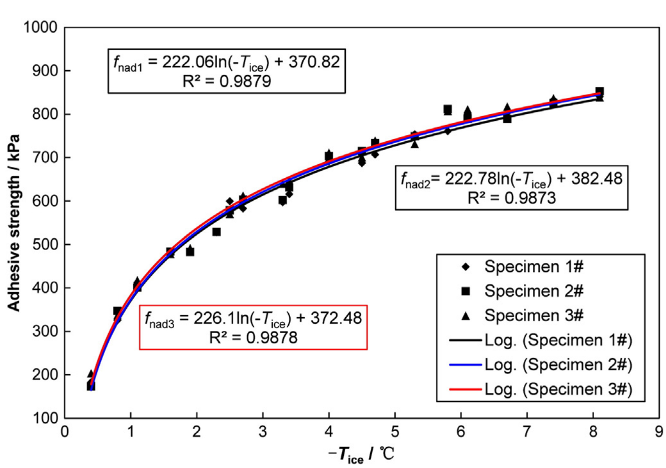

Fig. 9. Relationship between ice temperature and normal ice adhesive strength (the pavement MTD is about 0.65 mm).

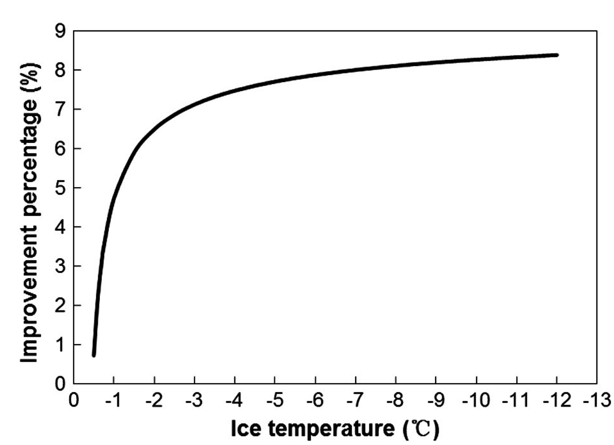

Fig. 11. Increase percentage of the normal ice adhesive strength for different ice temperatures.

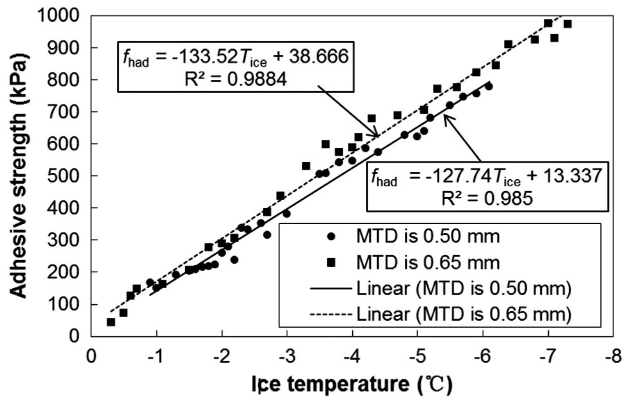

Fig. 12. Comparison of the relationship between ice temperature and horizontal ice adhesive strength for different pavement MTDs.

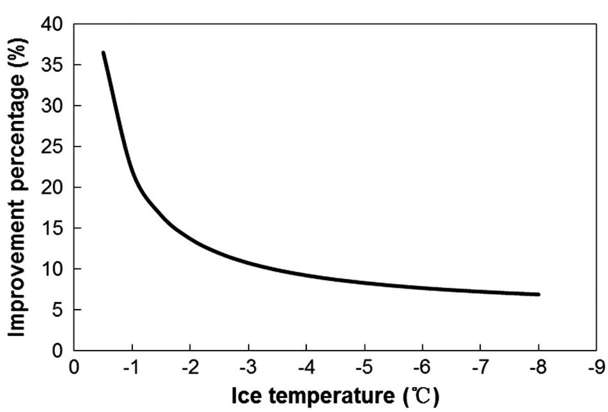

Fig. 13. Increase percentage of the horizontal ice adhesive strength for different ice temperatures.

showed the ice marks after test and it indicates that the ice mark area should be the exact contact area, but it is highly regrettable that the ice mark area cannot be obtained through experimental test in our laboratory. As a result, the ice contact area cannot be quantified through the experiment conducted in this paper. Nevertheless, to quantitatively weigh the weak and strong of the adhesive strength of ice to the asphalt pavement with various roughnesses, the mean texture depth should be taken into consideration in practical engineering. Accordingly, the adhesive force can be easily and conveniently evaluated for the specified area of the pavement surface with specified MTD. That is the required in practical engineering. Therefore, the current study has provided an important insight into the effects of ice temperature and MTD on the adhesive properties of ice to the asphalt pavement, and it shed light on the directions for future studies to investigate the adhesive properties of ice to other materials in civil engineering under the influence of ice temperature, roughness and other factors.

Acknowledgments

This research has been supported by the Fundamental Research Funds for the Central Universities of PR China (Grant No. 2012QNZT048), the National Natural Science Foundation (Grant No. 51248006) and the China Postdoctoral Science Foundation (Grant No. 2012M521563) to the first writer. The research is also assisted by the Special Financial Grant from the China Postdoctoral Science Foundation (Grant No. 2013T60865) and the National Natural Science Foundation (Grant No. 51308554).

References

Ahammed, M.A., Tighe, S., 2011. Asphalt pavements surface texture and skid resistance—exploring the reality. Can. J. Civ. Eng. 39, 1–9.
Andrews, E.H., Lockington, N.A., 1983. The cohesive and adhesive strength of ice. J. Mater. Sci. 18, 1455–1465.
Baker, H.R., Bascom, W.D., Singleterry, C.R., 1962. The adhesion of ice to lubricated surfaces. J. Colloid Sci. 17, 477–491.
Chu, M.C., Scavuzzo, R.J., 1991. Adhesive shear strength of impact ice. AIAA J. 29, 1921–1926.
Croutch, V.K., Harttey, R.A., 1992. Adhesion of ice to coatings and the performance of ice release coatings. J. Coatings Technol. 64, 41–52.
Dotan, A., Dodiuk, H., Laforte, C., Kenig, S., 2009. The relationship between water wetting and ice adhesion. J. Adhes. Sci. Technol. 23, 1907–1915.
Flintsch, G.W., León, E., McGhee, K.K., Al-Qadi, I.L., 2007. Pavement surface macrotexture measurement and applications. Transp. Res. Rec. 1860, 168–177.
Gustafson, K., 1982. Icing conditions on different pavement structures. Transp. Res. Rec. 860, 21–28.
Hanbali, R.M., 1994. Economic impact of winter road maintenance on road users. Transp. Res. Rec. 1442, 151–161.
Hassan, M.F., Lee, H.P., Lim, S.P., 2010. The variation of ice adhesion strength with substrate surface roughness. Meas. Sci. Technol. 21, 1–9.
Laforte, C., Beisswenger, A., 2005. Icephobic material centrifuge adhesion test. International Workshop on Atmospheric Icing of Structures (IWAIS XI), Montréal, June, pp. 1–5.
Laforte, C., Laforte, J.L., Carriere, J.C., 2002. How a solid coating can reduce the adhesion of ice on a structure. International Workshop on Atmospheric Icing of Structures (IWAIS), pp. 1–6.
Loughborough, D.L., 1946. Reduction of the adhesion of ice to de-icer surfaces. J. Aeronaut. Sci. 13, 126–134.
Maeno, N., 2004. Adhesion shear theory of ice friction at low sliding velocities, combined with ice sintering. J. Appl. Phys. 95, 134–139.
Matsumoto, K., Kobayashi, T., 2007. Fundamental study on adhesion of ice to cooling solid surface. Int. J. Refrig. 30, 851–860.
MoTPRC, 2012. Standard Test Methods of Bitumen and Bituminous Mixtures for Highway Engineering. China Communications Press, Beijing, China.
Oksanen, P., 1983. Friction and Adhesion of Ice. Technical Research Centre of Finland, Publication 10, Espoo (March, 36 pp.).
Ongel, A., Lu, Q., Harvey, J., 2009. Frictional properties of asphalt concrete mixes. Proc. ICE-Transp. 162, 19–26.
Petrenko, V.F., 1998. Effect of electric fields on adhesion of ice to mercury. J. Appl. Phys. 84, 261–267.
Petrenko, V.F., 1999. Reduction of ice adhesion to stainless steel by ice electrolysis. J. Appl. Phys. 86, 5450–5454.
Raraty, L.E., Tabor, D., 1958. The adhesion and strength properties of ice. Proc. R. Soc. A Math. Phys. Eng. Sci. 245, 184–201.
Ryzhkin, I.A., Petrenko, V.F., 1997. Physical mechanisms responsible for ice adhesion. J. Phys. Chem. B 101, 6267–6270.
Sarkar, D.K., Farzaneh, M., 2009. Superhydrophobic coatings with reduced ice adhesion. J. Adhes. Sci. Technol. 22, 1215–1237.
Tan, Y.Q., 2008. Deicing technologies for the pavement in the ice disaster. Transp. Constr. Manag. 49, 86–87.
Yang, X.D., Jin, J.F., 2002. Summary on mechanism of freezing adhesion and anti-freezing adhesion techniques and methods. J. Changchun Univ. Sci. Technol. 25, 17–19.
Yang, S., Kleehammer, D.M., Huo, Z., Sloan, E.D., Miller, K.T., 2004. Temperature dependence of particle-particle adherence forces in ice and clathrate hydrates. J. Colloid Interface Sci. 277, 335–341.
Zhu, Y.S., Xiang, H.L., Zhang, X.D., 2012. The skid resistance performance of the asphalt pavement under freezing condition. J. Wuhan Univ. Technol. (Transp. Sci. Eng) 36, 6–10.
Zou, M., Beckford, S., Wei, R., Ellis, C., Hatton, G., Miller, M.A., 2011. Effects of surface roughness and energy on ice adhesion strength. Appl. Surf. Sci. 257, 3786–3792.